Multipole expansion of the scattering of light from a metal microspheroid

Lan-chan Chu

Institute of Electronics, National Chiao Tung University, Hsinchu, Taiwan 300, China

Shou-yih Wang

Department of Physics, National Tsing Hua University, Hsinchu, Taiwan 300, China

Received September 18, 1984; accepted January 17, 1985

The scattering of light by a spheroidal metal particle has been newly treated by use of the technique of the multipole expansion of radiation fields from the induced polarization and the associated current and magnetization, which are now considered as radiation sources. The relation between the polarization and the incident field is most simply obtained by using the long-wavelength approximation and a radiation-damping correction. The various orders of electric- and magnetic-multipole coefficients of scattered fields have been separately calculated. Part of our calculated results confirm and thus justify the well-known features that the electric-dipole term gives the dominant contribution and that the magnitudes of multipole coefficients decrease monotonically with the increasing-order number of the multipoles. Some new features concerning the accuracy and the limitation of the radiation-damping correction are discussed against the depolarization factor of the spheroid. For a small sphere, the results reduce to the famous Rayleigh scattering, as expected. Results for larger spheres are compared with those of an exact electrodynamical calculation.

1. INTRODUCTION

Raman scattering by a molecule absorbed onto certain suitably roughened metal surfaces has been known for many years to be greatly enhanced.[1,2] Theories based on the electromagnetic local field arising from the bumpy surface are the most tractable and widely reported. The problem of surface-enhanced Raman scattering (SERS), however, is treated almost entirely in terms of only dipolar fields.[3,4] Even in the papers[5,6] that give more than the dipole term, the contributions from individual higher multipoles are not separated and cannot be compared with those of the dipole. In 1981, Liao *et al.*[4] fabricated lithographically isolated metal microspheroids and made an important advance in SERS studies through characterization of the roughness by isolated spheroids and affirmation of the electromagnetic model for the SERS. Since the size of the isolated spheroid was comparatively large (1500 Å in the semimajor axis), the higher-order multipole contributions should be relatively more pronounced. Barber *et al.*[5] have given an exact electrodynamic calculation, showing that the overall contribution of all higher multipoles is quite appreciable. Their method of calculation followed from that of Asano and Yamamoto,[7] which, based on the formal scattering theory of matching boundary values at the particle surface, neither clearly gives a separate contribution from each multipole nor provides a deeper physical insight owing to the complicated mathematics. The aim of this paper is to treat the light scattering by a new approach, namely, by using the existing technique of multipole expansion[8] in vector spherical harmonics and subsequently calculating the individual-multipole contribution in an easy fashion. The main feature of this approach, which presents direct physical insight into the calculation, lies in the use of the simple relation between the induced polarization of the spheroid and the incident electric field under the long-wavelength approximation and a radiation-damping correction. Although the SERS problem can be readily computed, we focus our attention only on the multipole expansion of an elastically scattered light field from an Ag spheroid. The formulation of the treatment is given in Section 2. The various results of individual multipole contributions and their dependence on the multipole-order number and the size of spheroid are given in Section 3. Comparisons in the cases of small and large spheres as well as other discussions and conclusions are also presented in Section 3.

2. FORMULATION

The scattering of light at optical frequencies by metal particles can be handled by using the same formulism as that of light scattering by dielectric particles.[9,10] We treat the scattering of light through two steps: (a) An incident light polarizes the microparticle (see Fig. 1), which in turn results in an induced polarization $\mathbf{P}(\mathbf{r}, t)$ and the associated polarization-charge density $\rho_p(\mathbf{r}, t) = -\nabla \cdot \mathbf{P}$, polarization-current density $\mathbf{J}_p(\mathbf{r}, t) = -(\partial \mathbf{P}/\partial t)$, and magnetization $\mathbf{M}_p(\mathbf{r}, t) = (1/2c)(\mathbf{r} \times \mathbf{J}_p)$. These quantities are then considered radiation sources. (b) The radiation fields arising from these radiation sources can be found by standard procedures. This two-step treatment was employed first by Chew *et al.*[11] and later by many authors in the calculation of the SERS.[12,13] But we note that, in these two-step treatments, most authors did not take into consideration the radiation damping that is due to the energy loss for the radiation from the time-varying source. In order to have more-accurate results, we will follow Wokaun *et al.*[14] and use a radiation-damping correction in our calculation.

As usual, we assume that the radiation sources are har-

0740-3224/85/060950-06$02.00

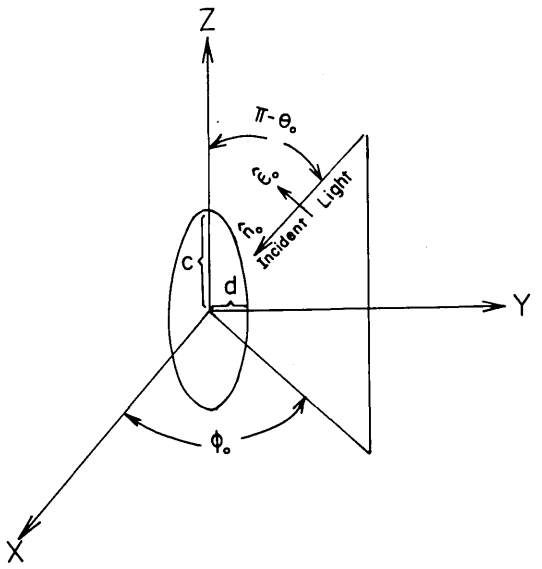

Fig. 1. The coordinate system of light scattering by an isolated prolate spheroid with semiminor axis d and semimajor axis c.

monically time varying. The Maxwell equations of $\mathbf{D}$ and $\mathbf{B}$ within the spheroid can then be written as

$$\nabla \cdot \mathbf{B} = 0, \tag{1}$$

$$\nabla \cdot \mathbf{D} = 0, \tag{2}$$

$$\nabla \times \mathbf{D} - ik\mathbf{B} = \frac{4\pi i}{\omega} \nabla \times \mathbf{J}_p, \tag{3}$$

$$\nabla \times \mathbf{B} + ik\mathbf{D} = 4\pi \nabla \times \mathbf{M}_p, \tag{4}$$

where $k = (\omega/c)$; c and ω are, respectively, the speed and the frequency of light in that medium. Note that the displacement vector $\mathbf{D}$ equals $\mathbf{E}$ outside the spheroidal particle.

The electric-multipole coefficients $a_E(l, m)$ of order (l, m) and the magnetic-multipole coefficients $a_M(l, m)$ of order (l, m) can be determined by Eqs. (16.91) and (16.92) of Ref. 8, if we replace ρ, $\mathbf{J}$, and $\mathbf{M}$ by ρ_p, $\mathbf{J}_p$, and $\mathbf{M}_p$, respectively, in these equations. The reason is that the above equations take exactly the same form as Eq. (16.84) of Ref. 8. Using $\nabla \cdot \mathbf{P} = -\rho_p$ inside the spheroid and $\mathbf{P} = 0$ outside the spheroid, we can write the coefficients in the following forms:

$$\begin{aligned} a_E(l, m) = \frac{4\pi k^2}{i\sqrt{l(l+1)}} \int \Bigg(& P_r \Big\{ k^2 r Y_{lm}^* j_l(kr) \\ & + Y_{lm}^* \frac{\partial^2}{\partial r^2} [r j_l(kr)] \Big\} \\ & + \Big\{ \frac{\partial}{\partial r} [r j_l(kr)] - \frac{k^2 r^2}{2} j_l(kr) \Big\} \Big(P_\theta \frac{\partial}{r \partial \theta} Y_{lm}^* \\ & + P_\phi \frac{1}{r \sin\theta} \frac{\partial}{\partial \phi} Y_{lm}^* \Big) \Bigg) \mathrm{d}^3 x, \end{aligned} \tag{5}$$

$$\begin{aligned} a_M(l, m) = \frac{4\pi k^3}{[l(l+1)]^{1/2}} \int & \Big\{ j_l(kr) + \tfrac{1}{2} \frac{\partial}{\partial r} [r j_l(kr)] \Big\} \\ & \times \Big[P_\theta \frac{1}{\sin\theta} \frac{\partial}{\partial \phi} Y_{lm}^* - P_\phi \frac{\partial}{\partial \theta} Y_{lm}^* \Big] \mathrm{d}^3 x, \end{aligned} \tag{6}$$

with

$$P_r = P_x \sin\theta \cos\phi + P_y \sin\theta \sin\phi + P_z \cos\theta, \tag{7}$$

$$P_\theta = P_x \cos\theta \cos\phi + P_y \cos\theta \sin\phi - P_z \sin\theta, \tag{8}$$

$$P_\phi = -P_x \sin\phi + P_y \cos\phi, \tag{9}$$

where P_r, P_θ, P_ϕ, P_x, P_y, and P_z are the spherical and the rectangular components of the polarization vector $\mathbf{P}$, respectively. Note that according to Ref. 8 the fields with harmonic time dependence ($e^{i\omega t}$, $\omega \neq 0$) will have no monopole terms, namely, $a_E(0, 0) = a_M(0, 0) = 0$.

It is tedious to find the formal relation between the polarization $\mathbf{P}$ and the incident field $\mathbf{E}_i$ by the matching boundary values.[7] For conceptual clarity and mathematical simplicity, we use the usual long-wavelength approximation with a correction of radiation damping.[14] This is valid when the ratio of spheroidal volume V to the cube of the wavelength λ of incident light is small compared with unity, which is consistent to our case. Thus we have for the incident field and the polarization[14]

$$\mathbf{E}_i = \hat{\epsilon}_0 E_0 \exp(ik\hat{n}_0 \cdot \mathbf{r}), \tag{10}$$

$$P_j = \frac{\epsilon - 1}{4\pi} \frac{(\hat{\epsilon}_0 E_0)_j}{1 - (1 - \epsilon)\left(A_j + i \frac{4}{3} \pi^2 \frac{V}{\lambda^3} \right)}, \qquad j = x, y, z, \tag{11}$$

where

$$\begin{aligned} A_x = A_y = & \frac{m}{2(m^2 - 1)} \\ & \times \left[m - \frac{1}{2(m^2 - 1)^{1/2}} \ln \frac{m + (m^2 - 1)^{1/2}}{m - (m^2 - 1)^{1/2}} \right], \end{aligned} \tag{12}$$

$$A_z = \frac{1}{m^2 - 1} \left[\frac{m}{2(m^2 - 1)^{1/2}} \ln \frac{m + (m^2 - 1)^{1/2}}{m - (m^2 - 1)^{1/2}} - 1 \right], \tag{13}$$

in which $m = c/d$; c, d, A_x, A_y, A_z, and ϵ are the semimajor and the semiminor axes, the depolarization-factor components[15] along the X, Y, and Z axes, and the dielectric constant[16] of the spheroid, respectively. Using Eqs. (7)–(9) and the following identities[17]:

$$\int_0^{2\pi} e^{-im\phi} \cos\phi \, \mathrm{d}\phi = \pi(\delta_{m,1} + \delta_{m,-1}), \tag{14}$$

$$\int_0^{2\pi} e^{-im\phi} \sin\phi \, \mathrm{d}\phi = \frac{\pi}{i}(\delta_{m,1} - \delta_{m,-1}), \tag{15}$$

$$\int_0^{2\pi} e^{-im\phi} \mathrm{d}\phi = 2\pi \delta_{m,0}, \tag{16}$$

$$\begin{aligned} \frac{\partial Y_{l,m}^*}{\partial \theta} = & \frac{1}{\sin\theta} \left[\frac{2l+1}{4\pi} \frac{(l-m)!}{(l+m)!} \right]^{1/2} e^{-im\phi} \\ & \times [(l+1)(-x)P_l^m \\ & + (l - m + 1)P_{l+1}^m], \end{aligned} \tag{17}$$

$$\frac{\partial Y_{l,m}^*}{\partial \phi} = -im Y_{lm}^*, \tag{18}$$

Eq. (5) becomes

$$\begin{aligned} a_E(l, m) = & \frac{k^2}{i} \left[\frac{4\pi}{l} \frac{(2l+1)}{(l+1)} \frac{(l-m)!}{(l+m)!} \right]^{1/2} \\ & \times [a_{E1}(l, m) + a_{E2}(l, m) + a_{E3}(l, m)], \end{aligned} \tag{19}$$

with

$$a_{E1}(l,m)=\pi\int_{-1}^{1}\left\{\left[P_x(\delta_{m,1}+\delta_{m,-1})+\frac{P_y}{i}(\delta_{m,1}-\delta_{m,-1})\right]\times(1-x^2)^{1/2}+2P_z x\delta_{m,0}\right\}\times\left(\int_0^{dc/[c^2+(d^2-c^2)x^2]^{1/2}}\left\{k^2 r j_l(kr)+\frac{\partial^2}{\partial r^2}[rj_l(kr)]\right\}r^2\mathrm{d}r\right)P_l^m(x)\mathrm{d}x, \tag{20}$$

$$a_{E2}(l,m)=\pi\int_{-1}^{1}\left\{\left[P_x(\delta_{m,1}+\delta_{m,-1})+\frac{P_y}{i}(\delta_{m,1}-\delta_{m,-1})\right]\times(1-x^2)^{1/2}-2P_z\delta_{m,0}\right\}\times\left(\int_0^{dc/[c^2+(d^2-c^2)x^2]^{1/2}}\times\left\{\frac{\partial}{\partial r}[rj_l(kr)]-\frac{k^2r^2}{2}j_l(kr)\right\}r\mathrm{d}r\right)\times[(-x)(l+1)P_l^m(x)+(l-m+1)P_{l+1}^m(x)]\mathrm{d}x, \tag{21}$$

$$a_{E3}(l,m)=im\pi\int_{-1}^{1}\left[\frac{P_x}{i}(\delta_{m,1}-\delta_{m,-1})-P_y(\delta_{m,1}+\delta_{m,-1})\right]\times\left(\int_0^{dc/[c^2+(d^2-c^2)x^2]^{1/2}}\left\{\frac{\partial}{\partial r}[rj_l(kr)]-\frac{k^2r^2}{2}j_l(kr)\right\}r\mathrm{d}r\right)\frac{P_l^m(x)\mathrm{d}x}{(1-x^2)^{1/2}}. \tag{22}$$

Equation (6) becomes

$$a_M(l,m)=\left[\frac{4\pi}{l}\frac{(2l+1)}{(l+1)}\frac{(l-m)!}{(l+m)!}\right]^{1/2}\times[a_{M1}(l,m)+a_{M2}(l,m)], \tag{23}$$

with

$$a_{M1}(l,m)=-im\pi\int_{-1}^{1}\left\{\left[P_x(\delta_{m,1}+\delta_{m,-1})+\frac{P_j}{i}(\delta_{m,1}-\delta_{m,-1})\right]\times\frac{x}{(1-x^2)^{1/2}}+2P_z\delta_{m,0}\right\}\times\left(\int_0^{dc/[c^2+(d^2-c^2)x^2]^{1/2}}\times\left\{j_l(kr)+\tfrac{1}{2}\frac{\partial}{\partial r}[rj_l(kr)]\right\}r^2\mathrm{d}r\right)P_l^m(x)\mathrm{d}x, \tag{24}$$

$$a_{M2}(l,m)=\pi\int_{-1}^{1}\left[\frac{P_x}{i}(\delta_{m,1}-\delta_{m,-1})-P_z(\delta_{m,1}+\delta_{m,-1})\right]\times\left(\int_0^{dc/[c^2+(d^2-c^2)x^2]^{1/2}}\times\left\{j_l(kr)+\tfrac{1}{2}\frac{\partial}{\partial r}[rj_l(kr)]\right\}r^2\mathrm{d}r\right)\times[(l+1)(-x)P_l^m(x)+(l-m+1)P_{l+1}^m(x)]\frac{\mathrm{d}x}{(1-x^2)^{1/2}}. \tag{25}$$

Using the property of evenness or oddness of $P_l^m(x)$ with respect to l and m, we can readily see from the above equations that $a_E(l,m)=0$ if l is even and that $a_M(l,m)=0$ if l is odd. The scattered fields $\mathbf{E}_{sc}$, $\mathbf{B}_{sc}$ outside the spheroid can be obtained in terms of $a_E(l,m)$ and $a_M(l,m)$ from Eq. (16.46) of Ref. 8 by setting $f_l(kr)=g_l(kr)=h_l^{(1)}(kr)$. The scattering cross section is as follows:

$$\sigma_s=\frac{1}{k^2E_0^2}\sum_{l,m}[|a_E(l,m)|^2+a_M(l,m)|^2]. \tag{26}$$

The scattering efficiency Q_{se} is customarily defined as the ratio of the scattered power to the incident power intercepted by a given geometrical cross section. For the case of a sphere[18] of radius a, it becomes

$$Q_{se}=\lim_{R\gg a}\frac{R^2}{\pi a^2E_0^2}\int_0^{2\pi}\int_0^{\pi}\mathbf{E}_{sc}\cdot\mathbf{E}_{sc}^{*}\sin\theta\mathrm{d}\theta\mathrm{d}\phi, \tag{27}$$

where R denotes the radial position of the observation point. The relation between σ_s and Q_{se} in the case of a sphere is

$$Q_{se}=\frac{\sigma_s}{\pi a^2}=\frac{1}{\pi(ka)^2E_0^2}\sum_{l,m}[|a_E(l,m)|^2+|a_M(l,m)|^2]. \tag{28}$$

Now we take the special case of a small sphere ($ka\ll 1$) with the electric-dipole moment along the z direction ($l=1, m=0$). The coefficient $a_E(1,0)$ can be found by Eqs. (11) and (19) to be

$$a_E(1,0)=-\left(\frac{8\pi}{3}\right)^{1/2}k^3\frac{\epsilon-1}{\epsilon+2}a^3E_z, \tag{29}$$

where E_z is the z component of applied field $\mathbf{E}_i$ with amplitude E_0. The scattering cross section for this case is obtained from Eq. (26):

$$\sigma_s=\frac{8\pi}{3}\left|\frac{\epsilon-1}{\epsilon+2}\right|^2k^4a^6, \tag{30}$$

which is, just as expected, the scattering cross section of Rayleigh scattering of light by a small sphere.[8,19]

3. NUMERICAL RESULTS AND DISCUSSIONS

We consider only a p-polarized wave incident upon a homogeneous prolate spheroid, since the usual treatment of the EM model of a SERS problem assumes that only the z component of the electric-dipole moment of the molecule is Raman active.[3,13,14] The propagation unit vector $\hat{n}_0$ and the polarization with vector $\hat{\epsilon}_0$ of the incident light can be written as

$$\hat{n}_0=(\sin\theta_0\cos\phi_0,\sin\theta_0\sin\phi_0,\cos\theta_0), \tag{31}$$

$$\hat{\epsilon}_0=(\cos\theta_0\cos\phi_0,\cos\theta_0\sin\phi_0,-\sin\theta_0), \tag{32}$$

where θ_0 and ϕ_0 are spherical angles. The numerical results of electric- and magnetic-multipole coefficients from a spheroidal microparticle polarized by light have been calculated by using the above equations and compared for three different particle sizes: $d=167$ Å and $c=500$ Å for an arbitrary choice of small size with aspect ratio 3:1, $d=263$ Å and $c=993$ Å for an optimum choice[20] in accord with the experimental data of Liao *et al.*[4], and $d=500$ Å and $c=1500$ Å for the formed size of that experiment.[4] These numerical results

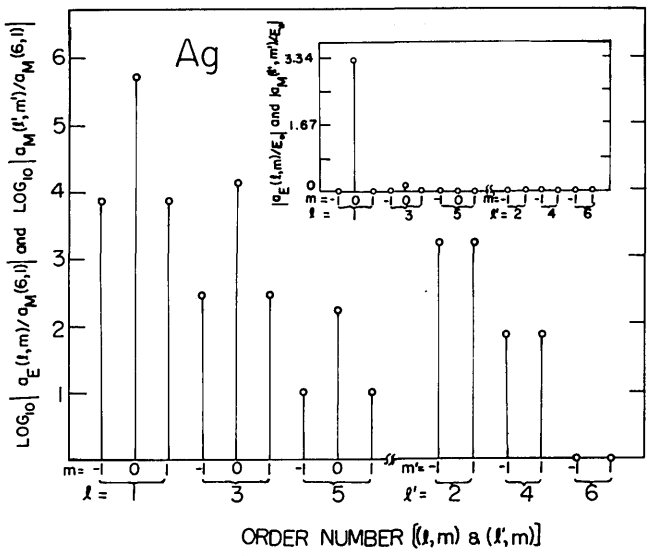

Fig. 2. The logarithmic scale normalized to $|a_M(6,1)|$ and the linear scale (inset) of the magnitude of electric- and magnetic-multipole coefficients of the Ag spheroidal particle versus the mutipole-order numbers (l, m) with $d = 263$ Å, $c = 993$ Å; $\theta_0 = 60°$, $\phi_0 = 0°$; photon energy, 2.55 eV.

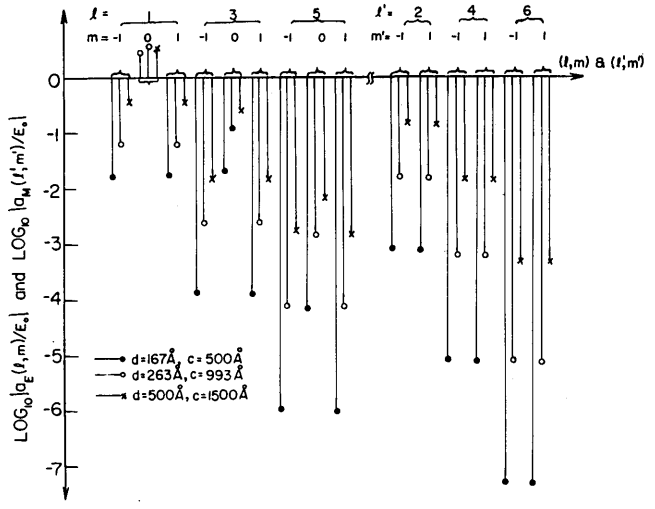

Fig. 3. The logarithmic scale of the magnitude of electric- and magnetic-multipole coefficients of the Ag spheroidal particle versus the multipole-order numbers (l, m) for various sizes. $d = 167$ Å, $c = 500$ Å; $d = 263$ Å, $c = 993$ Å; and $d = 500$ Å, $c = 1500$ Å with $\theta_0 = 60°$, $\phi_0 = 0°$; photon energy, 2.55 eV.

are plotted in Figs. 2 and 3. The plots indicate that the electric-dipole coefficient $a_E(1, 0)$ offers the principal contribution to the scattering field, and the magnitudes of other multipole coefficients drop strikingly with increasing-order numbers. Figure 3 also displays that each higher-order multipole coefficients (same l, m) becomes more important with increasing particle volume. It gives a more pronounced contribution to scattered fields for a large-size particle. These results are known and are confirmed or justified by this calculation. We emphasize that, for any l, the electric-multipole coefficients $a_E(l, m)$ are nonvanishing only for $m = 0 \pm 1$ and that, for magnetic-multipole coefficients $a_M(l, m)$, only the multipoles $m = \pm 1$ exist, as is shown in Figs. 2 and 3. Figures 4 and 5 are the plots with different photon energies and polar angles of incident light. There are some changes, but these are not so substantial in the multipole coefficients. To a large extent, similar features have been found for Au.

In order to understand the accuracy and the limitation of our approach, we now work on the validity of the radiation damping from Eq. (11) and set

$$B = \frac{4}{3}\pi^2 \frac{V}{\lambda^3}, \tag{33}$$

$$\epsilon = \epsilon_1 + i\epsilon_2. \tag{34}$$

To be specific, we consider the case of Ag in which the imaginary part ϵ_2 of ϵ is small (≤ 0.5), whereas the real part ϵ_1 of ϵ decreases from -2 to -40 over the range 3.5–1.39 eV.[16] Equation (11) then becomes

$$P_j = \frac{\epsilon - 1}{4\pi} \frac{1}{1 - (1 - \epsilon_1)A_j + B\epsilon_2 + i[(1 - \epsilon_1)B - A_j\epsilon_2]}. \tag{35}$$

Particle plasmon resonance should occur when the real part of denominator of Eq. (35) vanishes, namely, $1 - (1 - \epsilon_1)A_j + B\epsilon_2 = 0$. We discuss two cases:

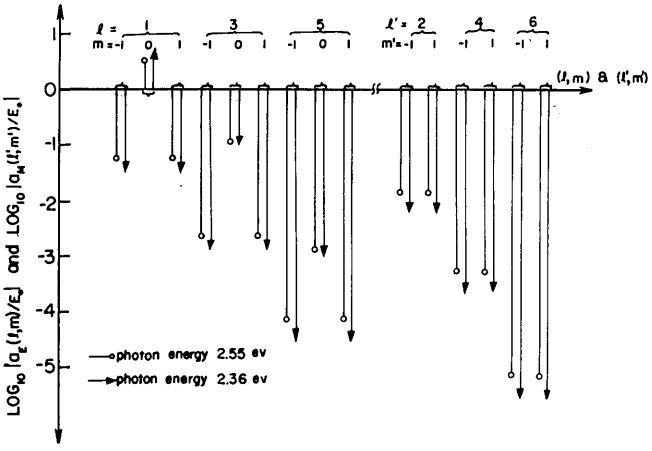

Fig. 4. The logarithmic scale of the magnitude of electric- and magnetic-multipole coefficients of the Ag spheroidal particle versus multipole-order numbers (l, m) with different energies 2.55 and 2.36 eV for $d = 263$ Å, $c = 993$ Å, $\theta_0 = 60°$, and $\phi_0 = 0°$.

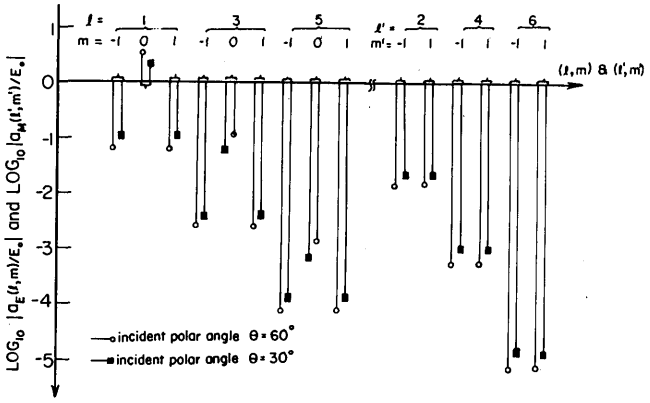

Fig. 5. The logarithmic scale of the magnitude of electric- and magnetic-multipole coefficients of the Ag spheroidal particle versus mutipole-order numbers (l, m) with different incident polar angles $\theta_0 = 60°$ and $\theta_0 = 30°$ for $\phi_0 = 0°$, $d = 263$ Å, and $c = 993$ Å; photon energy, 2.55 eV.

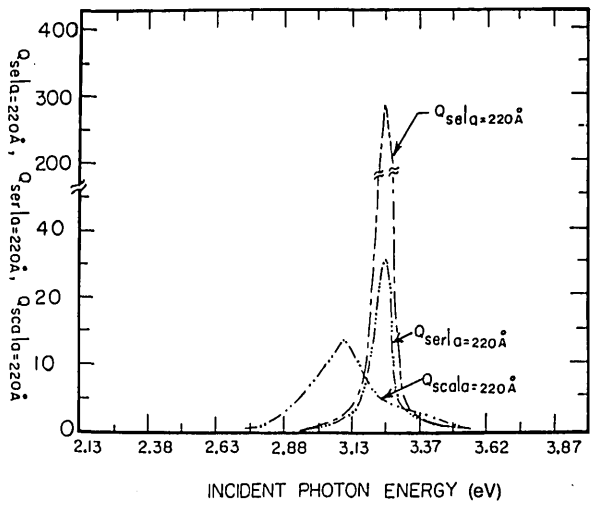

Fig. 6. Comparison of the calculated scattering efficiency Q_{se} versus incident photon energies with the well-known Rayleigh result denoted as Q_{ser} and with those of the exact solution of Ref. 18 denoted as Q_{sca}, for a sphere immersed in water with radius $a = 220$ Å.

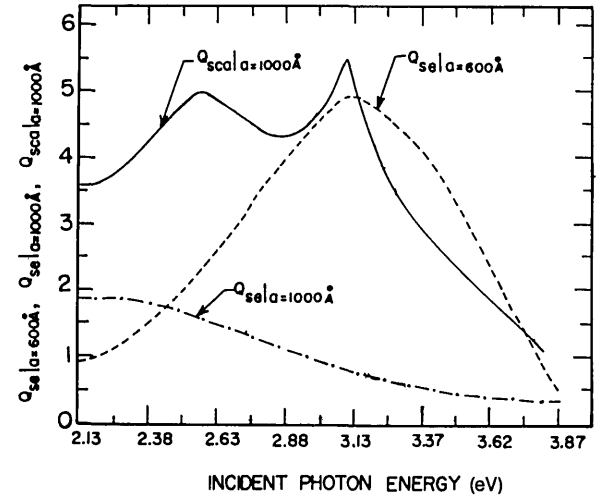

Fig. 7. Comparison of the calculated scattering efficiency Q_{se} versus incident photon energy with those of the exact solution of Ref. 18 denoted as Q_{sca} for a sphere immersed in water with radius $a = 600$ Å and $a = 1000$ Å, respectively.

Case 1: $A_j \gg B$. Equation (35) reduces to the resonant polarization

$$(P_j)_{res} = \frac{\epsilon_{res} - 1}{4\pi} \frac{1}{i[(1-\epsilon_1)B - A_j\epsilon_2]}. \tag{36}$$

In this case, one may have very small B such that

$$(1-\epsilon_1)B \ll A_j\epsilon_2.$$

Clearly this reduces to the famous Rayleigh scattering. Since $(1-\epsilon_1)$ can be quite large for Ag, one may still obtain the relation

$$(1-\epsilon_1)B \sim A_j\epsilon_2.$$

This can give the result that $|(P_j)_{res}|$ becomes greater than the resonant polarization without using radiation damping. This feature is clearly manifested in the case of a sphere of radius $a = 220$ Å immersed in water, as is shown in Fig. 6, for which $(1-\epsilon_1)B = 0.047$ and $A_j\epsilon_2 = 0.061$ for the resonance peak with a photon energy of 3.25 eV.

Case 2: B is comparable with A_j. Equation (37), owing to small ϵ_2, becomes

$$(P_j)_{res} = \frac{\epsilon_{res} - 1}{4\pi} \frac{1}{i[(1-\epsilon_1)B]}. \tag{37}$$

In this case, the magnitude of $(P_j)_{res}$ decreases with increasing B, as is shown in Fig. 7 for the sphere of radius $a = 600$ Å immersed in water. The broadening resulting from the radiation damping is rather striking. When the radiation-damping term B is larger than A_j, the broadening effect would be too large to apply the radiation-damping technique as a first-order correction[5] treatment. We plotted the results of Q_{se} in Fig. 7 for $a = 1000$ Å to demonstrate this property.

Finally, we compare our results with those for the case of a sphere immersed in water, which has been solved exactly by Messinger *et al.*[18] using the Maxwell equations. We take $c = d = a$ as the sphere case, replace ϵ by $\epsilon/1.77$ for the water environment, and use various sizes to compare the scattering efficiency Q_{se} with the Q_{sca} of Messinger *et al.* These are shown in Fig. 6. For small size of a sphere with $a = 220$ Å, the scattering efficiency $Q_{se}|_{a=220Å}$ calculated by Eq. (28) including the radiation-damping correction has the same peak position at 3.25 eV but differs in magnitude from that of Rayleigh scattering denoted by $Q_{ser}|_{a=220Å}$. This increase in Q_{se} at resonance corresponds to the increase in $|(P_j)_{res}|$. The reason for the increase has been explained in case 1 above. When we neglect the radiation-damping term B, we obtain exactly the Rayleigh-scattering result. We notice that the scattering efficiency $Q_{sca}|_{a=220Å}$ of the exact electrodynamic solution,[18] when compared with the Rayleigh $Q_{ser}|_{a=220Å}$, has smaller magnitude and a shift of resonance peak, probably because of phase-retardation effects. In this case, we have $A_j \gg B$ ($A_j = 0.333 \gg B = 1.05 \times 10^{-2}$ at 3.25 eV). The salient feature is that there is only one sharp resonance. Next is the case of such large sphere volume that B (0.21 at 3.25 eV) is comparable with A_j, with $a = 600$ Å, for example, shown in Fig. 7. The curve of scattering efficiency $Q_{se}|_{a=600Å}$ versus photon energies has broadened linewidth and decreased magnitude, as mentioned before. The features in Fig. 7 are similar to those of phase-retardation effects in an electrodynamical calculation made by Meier and Wokaun.[21] This is rather in accord with their idea[21] that the consideration of phase retardation would give the effect of radiation damping. If we take $a = 1000$ Å ($B = 0.99$ at 3.25 eV) and use Eq. (28), there is apparently no resonant feature within the range 2.31–3.87 eV. The plot differs largely from that of the exact electrodynamic calculation by Messinger *et al.* (denoted by $Q_{sca}|_{a=1000Å}$). As mentioned above, this lack of sharp resonance would result from the invalidity of using such large radiation damping as a first-order correction.[5]

To conclude, we have calculated with a new technique the multipole expansion of the light scattering from a metal particle by using the long-wavelength approximation and the radiation-damping correction. The results, apart from the well-known dominating features of the electric-dipole term over the other multipoles, have revealed that, for a small spheroidal size such that $(1-\epsilon_1)B \sim A_j\epsilon_2$, the radiation-damping correction could yield enhancement rather than damping. For large sizes ($B > A_j$), the resonance peak in the excitation profile should disappear. For small sizes of spheres

our results are compared with Rayleigh scattering, and for larger spheres other existing exact electrodynamical calculations are discussed.

ACKNOWLEDGMENT

This research was financially sponsored by the National Science Council, Taiwan.

REFERENCES

1. M. Fleischmann, P. J. Hendra, and A. J. McQuillan, "Raman spectra of pyridine adsorbed at a silver electrode," Chem. Phys. Lett. **26,** 163 (1974).
2. R. K. Chang and T. E. Furtak, *Surface Enhanced Raman Scattering* (Plenum, New York, 1982).
3. J. Gersten and A. Nitzan, "Electromagnetic theory of enhanced Raman scattering by molecules adsorbed on rough surfaces," J. Chem. Phys. **73,** 3023 (1980).
4. P. F. Liao, J. G. Bergman, D. S. Chemla, A. Wokaun, J. Melngailis, A. M. Hawryluk, and N. P. Economou, "Surface-enhanced Raman scattering from microlithographic silver particle surfaces," Chem. Phys. Lett. **82,** 355 (1981).
5. P. W. Barber, R. K. Chang, and H. Massoudi, "Surface enhanced electric intensities on large silver spheroids," Phys. Rev. Lett. **50,** 997 (1983).
6. M. Kerker, D.-S. Wang, and H. Chew, "Surface enhanced Raman scattering (SERS) by molecules adsorbed at spherical particles: errata," Appl. Opt. **19,** 4159 (1980).
7. S. Asano and G. Yamamoto, "Light scattering by a spheroidal particle," Appl. Opt. **14,** 29 (1975).
8. J. D. Jackson, *Classical Electrodynamics* (Wiley, New York, 1975), pp. 394, 414, 739–776.
9. H. C. van de Hulst, *Light Scattering by Small Particles* (Wiley, New York, 1957).
10. M. Kerker, *The Scattering of Light and Other Electromagnetic Radiation* (Academic, New York, 1969).
11. H. Chew, P. J. McNulty, and M. Kerker, "Model for Raman and fluorescent scattering by molecules embedded in small particles," Phys. Rev. A **13,** 396 (1976).
12. S. L. McCall, P. M. Platzman, and P. A. Wolff, "Surface enhanced Raman scattering," Phys. Lett. **77A,** 381 (1980); D.-S. Wang and M. Kerker, "Enhanced Raman scattering by molecules absorbed at the surface of colloidal spheroids," Phys. Rev. B **24,** 1777 (1981).
13. M. Inoue and K. Ohtaka, "Enhanced Raman scattering by two-dimensional array of polarizable spheres," J. Phys. Soc. Jpn. **52,** 1457 (1983).
14. A. Wokaun, J. P. Gordon, and P. F. Liao, "Radiation damping in surface-enhanced Raman scattering," Phys. Rev. Lett. **48,** 957 (1982).
15. J. A. Osborn, "Demagnetizing factors of the general ellipsoid," Phys. Rev. **67,** 351 (1945).
16. P. B. Johnson and R. W. Christy, "Optical constants of the noble metals," Phys. Rev. B **6,** 4370 (1972).
17. P. M. Morse and H. Feshbach, *Methods of Theoretical Physics* (McGraw-Hill, New York, 1953), p. 1326.
18. B. J. Messinger, K. U. von Raben, and R. K. Chang, "Local fields at the surface of noble-metal microspheres," Phys. Rev. B **24,** 649 (1981).
19. L. P. Bayvel and A. R. Jones, *Electromagnetic Scattering and Its Applications* (Applied Science, London, 1981), p. 48.
20. L. C. Chu and S. Y. Wang, "The contributions of r^{-1}, r^{-2}, r^{-3} terms of the full dipole fields associated with Raman scattering enhancement from CN molecules adsorbed on a 2-D array of Ag spheroids," J. Appl. Phys. (to be published).
21. M. Meier and A. Wokaun, "Enhanced fields on large metal particles: dynamical depolarization," Opt. Lett. **8,** 581 (1983).